The Emerald Research Register for this journal is available at
www.emeraldinsight.com/researchregister

The current issue and full text archive of this journal is available at
www.emeraldinsight.com/0961-5539.htm

Fin placement for optimal forced convection heat transfer from a cylinder in cross-flow

Bassam A/K Abu-Hijleh

School of Aerospace, Mechanical and Manufacturing Engineering, RMIT University, Victoria, Australia

Received February 2003
Accepted February 2004

Abstract

Purpose – The aim of this work is to determine the optimal number and location of the fin(s) for maximum laminar forced convection heat transfer from a cylinder with multiple high conductivity radial fins on its outer surface in cross-flow, i.e. Nusselt number, over a range of Reynolds numbers.

Design/methodology/approach – The effect of several combinations of number of fins, fin height, and fin(s) tangential location on the average Nusselt number was studied over the range of Reynolds numbers (5-150). The problem was investigated numerically using finite difference method over a stretched grid. The optimal number and placement of the fins, for maximum Nusselt number, was determined for several combinations of Reynolds number and fin height. The percentage improvement in heat transfer per fin(s) unit length, i.e. cost-efficiency, was also studied.

Findings – The results indicate that the fin(s) combination with the highest normalised Nusselt number is not necessarily the combination that results in the highest fin cost-efficiency.

Originality/value – The results of the study can be used to design highly efficient cross-flow forced convection heat transfer configurations from a horizontal cylinder with minimum cost.

Keywords Convection, Numerical analysis, Geometric planes and solids

Paper type Research paper

Nomenclature

D = cylinder diameter, $2r_0$ (m)
E = parameter in computational domain, $\pi e^{\pi\xi}$
F = number of fins
g = gravity (m/s^2)
H = non-dimensional fin height, h_f/r_o
h = local convection heat transfer coefficient (W/m^2 K)
h_f = fin height (m)
k = conduction heat transfer coefficient (W/m K)
M = number of grid points in the tangential direction
N = number of grid points in the radial direction
Nu_D = local Nusselt number based on cylinder diameter
$\overline{\mathrm{Nu}_D}$ = average Nusselt number based on cylinder diameter for a smooth cylinder, no fins
$\overline{\mathrm{Nu}_{D,F}}$ = average Nusselt number based on cylinder diameter, cylinder with F number of fins
$\overline{\mathrm{NU}_{D,F}}$ = normalized Nusselt number, equation (11)
P = non-dimensional pressure
p = pressure (Pa)
Pr = Prandtl number
R = non-dimensional radius
r = radius (m)
Re = Reynolds number based on cylinder radius, $U_\infty r_o/\nu$
Re_D = Reynolds number based on cylinder diameter, $U_\infty D/\nu = 2\mathrm{Re}$
T = temperature (K)
U = non-dimensional radial velocity

International Journal for Numerical Methods in Heat & Fluid Flow
Vol. 15 No. 3, 2005
pp. 277-295

0961-5539
DOI 10.1108/09615530510583892

u = radial velocity (m/s)
V = non-dimensional tangential velocity
v = tangential velocity (m/s)
α = thermal diffusivity (m^2/s)
β = coefficient of thermal expansion (K^{-1})
$\in$ = measure of convergence of numerical results
η = independent parameter in computational domain representing tangential direction
η_{fc} = percentage fin "cost-efficiency", equation (12)
θ = angle (degrees)
ν = kinematic viscosity (m^2/s)
ξ = independent parameter in computational domain representing radial direction
ρ = density (kg/m^3)
ϕ = non-dimensional temperature
ψ = stream function
ω = vorticity function

Subscripts

D = value based on cylinder diameter
f = value at fin
0 = value at cylinder surface
∞ = free stream value
1 = value for the fixed first fin, in the two non-uniformly spaced fins configurations
2 = value for the second fin, in the two non-uniformly spaced fins configurations

Introduction

Laminar forced convection across a heated cylinder is an important problem in heat transfer. It is used to simulate a wide range of engineering applications as well as to provide a better insight into more complex systems of heat transfer. Accurate knowledge of the convection heat transfer around circular cylinders is important in many fields, including heat exchangers, hot water and steam pipes, heaters, refrigerators and electrical conductors. Because of its industrial importance, this class of heat transfer has been the subject of many experimental and analytical studies. Though a lot of work has been done in this area, it still remains the subject of many investigations. Recent economic and environmental concerns have raised the interest in methods of increasing or reducing the convection heat transfer, depending on the application, from a horizontal cylinder. Researchers continue to look for new methods of heat transfer control. The use of porous materials to alter the heat transfer characteristics has been reported by several researchers including Vafai and Huang (1994), Al-Nimr and Alkam (1998) and Abu-Hijleh (2001).

Fins have always been used as a passive method of enhancing the convection heat transfer from cylinder (Ahmad, 1996). Previous work by the author has shown that increasing the number of uniformly spaced fins beyond a Reynolds number dependent value does not result in further enhancement in the convection heat transfer and can even result in a reduction in the Nusselt number (Abu-Hijleh, 2003). No published work could be located that discusses the selective, non-uniformly spaced, placement of fins for maximum forced convection heat transfer from a horizontal cylinder. This paper details the changes in the Nusselt number due to the use of one or more high conductivity fin(s) placed at different locations around the cylinder's outer surface. The aim is to establish the optimal configuration for maximum heat transfer as well as the optimal configuration for maximum return on the cost of using the fins. The fluid under consideration is air. The elliptic momentum and energy equations were solved numerically using the stream function-vorticity method on a stretched grid. This study included varying the Reynolds number from 5 to 150, number of fins from 1 to 11, and the non-dimensional fin height from 0.25 to 2.0. This range of values was based on the

experience gained from a previous work using uniformly spaced fins for the same configuration (Abu-Hijleh, 2003). Owing to symmetry, the computations were carried on half the physical domain making use of the horizontal symmetry passing through the center of the cylinder. The number of fins reported herein is for half a cylinder, due to symmetry, and should be doubled for a complete cylinder. No fins were located on the symmetry plane.

Mathematical analysis

The steady-state equations for 2D laminar forced convection over a horizontal cylinder are given by:

$$\frac{1}{r}\frac{\partial(ru)}{\partial r}+\frac{1}{\mathrm{r}}\frac{\partial v}{\partial \theta}=0 \tag{1}$$

$$u\frac{\partial u}{\partial r}+\frac{v}{r}\frac{\partial u}{\partial \theta}-\frac{v^2}{r}=-\frac{1}{\rho}\frac{\partial p}{\partial r}+\nu\left[\frac{\partial^2 u}{\partial r^2}+\frac{1}{r}\frac{\partial u}{\partial r}-\frac{u}{r^2}+\frac{1}{r^2}\frac{\partial^2 u}{\partial \theta^2}-\frac{2}{r^2}\frac{\partial v}{\partial \theta}\right] \tag{2}$$

$$u\frac{\partial v}{\partial r}+\frac{v}{r}\frac{\partial v}{\partial \theta}+\frac{uv}{r}=-\frac{1}{\rho}\frac{\partial p}{\partial r}+\nu\left[\frac{\partial^2 v}{\partial r^2}+\frac{1}{r}\frac{\partial v}{\partial r}-\frac{v}{r^2}+\frac{1}{r^2}\frac{\partial^2 v}{\partial \theta^2}+\frac{2}{r^2}\frac{\partial u}{\partial \theta}\right] \tag{3}$$

$$u\frac{\partial T}{\partial r}+\frac{v}{r}\frac{\partial T}{\partial \theta}=\alpha\nabla^2 T \tag{4}$$

where

$$\nabla^2 \equiv \left[\frac{\partial^2}{\partial r^2}+\frac{1}{r}\frac{\partial}{\partial r}+\frac{1}{r^2}\frac{\partial^2}{\partial \theta^2}\right]$$

Equations (1)-(4) are subject to the following boundary conditions.

(1) On the cylinder surface, i.e. $r = r_0$; $u = v = 0$ and $T = T_0$.

(2) Far-stream from the cylinder, i.e. $r \rightarrow \infty$; $u \rightarrow U_\infty \cos\theta$ and $v \rightarrow -U_\infty \sin\theta$. As for the temperature, the far-stream boundary condition is divided into an outflow ($\theta \leq 90°$) and an inflow ($\theta > 90°$) regions (Figure 1). The far-stream temperature boundary conditions are $T = T_\infty$ and $\partial T/\partial r = 0$ for the inflow and outflow regions, respectively.

(3) Plane of symmetry; $\theta = 0$ and $180°$ $v = 0$ and $\partial u/\partial\theta = \partial T/\partial\theta = 0$.

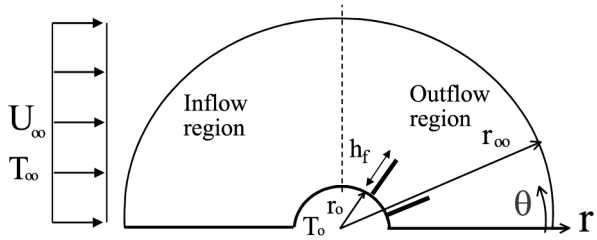

Figure 1.
Schematic of the cylinder, showing a non-uniformly spaced fins case

(4) On the fin surface; $u = v = 0$. Since the fins are assumed to be very thin and of very high conductivity, the temperature at any point along the fin will be that of the cylinder surface, i.e. $T_f = T_0$. The fins are equally spaced around the perimeter of the cylinder. No fins were placed on the horizontal plane of symmetry, i.e. at $\theta = 0$ and 180° (Figure 2).

In actual applications, the fin's temperature will vary along its radial distance and the variation will depend on the thickness and conductivity of the fin. But this gives rise to a conjugated heat transfer problem where the conduction heat transfer in the fin and the convection heat transfer in the surrounding air need to be solved simultaneously. This will greatly complicate the solution process. The assumption of constant fin temperature used in boundary condition 4 is intended to cancel the need to solve the conjugated heat transfer problem. Future work will try to address this issue and ascertain the effect of using "real" fin properties.

The local Nusselt number, based on diameter, on the cylinder surface is given by:

$$\mathrm{Nu}_D(\theta) = \frac{Dh(\theta)}{k} = -\frac{D}{(T_0 - T_\infty)} \frac{\partial T(r_0, \theta)}{\partial r} \tag{5}$$

The local Nusselt number at fin, based on diameter, is given by:

$$\mathrm{Nu}_{D,F}(\theta) = \int_1^{1+h_f} -\frac{D}{(T_o - T_\infty)} \frac{1}{r} \left[\left. \frac{\partial T(r, \theta)}{\partial r} \right|_{\mathrm{top}} + \left. \frac{\partial T(r, \theta)}{\partial r} \right|_{\mathrm{bottom}} \right] \mathrm{d}r \tag{6}$$

The following non-dimensional groups are introduced:

$$R \equiv \frac{r}{r_0}, \quad U \equiv \frac{u}{U_\infty}, \quad V \equiv \frac{v}{U_\infty}, \quad \phi \equiv \frac{(T - T_\infty)}{(T_0 - T_\infty)}, \quad P \equiv \frac{(p - p_\infty)}{\frac{1}{2}\rho U_\infty^2}$$

Using the stream function-vorticity formulation, the non-dimensional forms of equations (1)-(4) are given by (Anderson, 1994):

$$\omega = \nabla^2 \psi \tag{7}$$

$$U \frac{\partial \omega}{\partial R} + \frac{V}{R} \frac{\partial \omega}{\partial \theta} = \frac{1}{\mathrm{Re}} \nabla^2 \omega \tag{8}$$

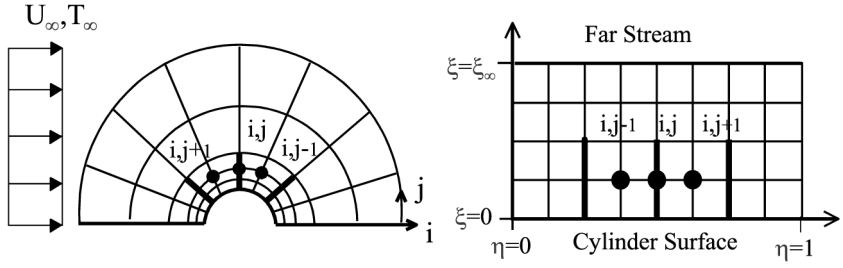

Figure 2.
Schematic of the grid in the physical (left) and computational (right) domains, showing a uniformly spaced fins case

$$U\frac{\partial\phi}{\partial R}+\frac{V}{R}\frac{\partial\phi}{\partial\theta}=\frac{1}{\mathrm{Re}\,\mathrm{Pr}}\nabla^2\phi \tag{9}$$

where

$$U\equiv\frac{1}{R}\frac{\partial\psi}{\partial\theta},\quad V\equiv-\frac{\partial\psi}{\partial R},\quad \mathrm{Re}=\frac{U_\infty r_o}{\nu},\quad \mathrm{Re}_D=\frac{U_\infty D}{\nu},\quad \mathrm{Pr}=\frac{\nu}{\alpha} \tag{10}$$

The new non-dimensional boundary conditions for equations (7)-(9) are given by:

(1) on the cylinder surface, i.e. $R=1.0$; $\psi=\partial\psi/\partial R=0$, $\omega=\partial^2\psi/\partial R^2$, and $\phi=1.0$;

(2) far-stream from the cylinder, i.e. $R\rightarrow\infty$; $(\partial\psi/\partial R)=\sin\theta$ and $(1/R)(\partial\psi/\partial\theta)=\cos\theta$. For the non-dimensional temperature, $\phi=0$ and $\partial\phi/\partial R=0$, for the inflow and outflow regions, respectively;

(3) plane of symmetry; $\psi=\omega=\partial\phi/\partial\theta=0$; and

(4) on the fin surface; $\psi=0$, $\omega=(1/R^2)(\partial^2\psi/\partial\theta^2)$, and $\phi_{ij}=1.0$.

The effect of adding the fin(s) on the convection heat transfer from the cylinder will be presented in terms of the normalized Nusselt number ($\overline{\mathrm{NU}_{D,F}}$) and the percentage fin "cost-efficiency" (η_{fc}), as per equations (11) and (12) shown below. The first term shows the relative change in the Nusselt number while the second shows the percentage relative change in the Nusselt number per unit length of fin(s) used. The percentage fin "cost-efficiency" should not be confused with the standard definition of fin efficiency or effectiveness. This parameter is intended to give an idea about the economic return of using the fin(s).

$$\overline{\mathrm{NU}_{D,F}}=\frac{\overline{\mathrm{NU}_{D,F}}}{\overline{\mathrm{NU}_D}} \tag{11}$$

$$\eta_{\mathrm{fc}}(\mathrm{per\ \ cent})=\frac{(\overline{\mathrm{NU}_{D,F}}-1)}{FH}\times 100 \tag{12}$$

In order to accurately resolve the boundary layer around the cylinder, a grid with small radial spacing is required. It is not practical to use this small spacing as we move to the far-stream boundary. Thus a stretched grid in the radial direction is needed (Anderson, 1994). This will result in unequally spaced nodes and would require the use of more complicated and/or less accurate finite difference formulas. To overcome this problem, the unequally spaced grid in the physical domain (R,θ) is transformed into an equally spaced grid in the computational domain (ξ,η) (Anderson, 1994) (Figure 2). The two domains are related as follows:

$$R=\mathrm{e}^{\pi\xi},\quad \theta=\pi\eta \tag{13}$$

Equations (7)-(9) along with the corresponding boundary conditions need to be transformed into the computational domain. In the new computational domain, the current problem will be given by:

$$\omega=\frac{1}{E^2}\left[\frac{\partial^2\psi}{\partial\xi^2}+\frac{\partial^2\psi}{\partial\eta^2}\right] \tag{14}$$

$$\frac{\partial^2 \omega}{\partial \xi^2} + \frac{\partial^2 \omega}{\partial \eta^2} = \mathrm{Re}\left[\frac{\partial \psi}{\partial \eta}\frac{\partial \omega}{\partial \xi} - \frac{\partial \psi}{\partial \xi}\frac{\partial \omega}{\partial \eta}\right] \tag{15}$$

$$\frac{\partial^2 \phi}{\partial \xi^2} + \frac{\partial^2 \phi}{\partial \eta^2} = \mathrm{Re}\,\mathrm{Pr}\left[\frac{\partial \psi}{\partial \eta}\frac{\partial \phi}{\partial \xi} - \frac{\partial \psi}{\partial \xi}\frac{\partial \phi}{\partial \eta}\right] \tag{16}$$

where

$$E = \pi e^{\pi \xi} \tag{17}$$

The transformed boundary conditions are given by:

(1) on the cylinder surface, i.e. $\xi = 0$; $\psi = \partial\psi/\partial\xi = 0$, $\omega = (1/\pi^2)(\partial^2\psi/\partial\xi^2)$, and $\phi = 1.0$;

(2) far-stream from the cylinder, i.e. $\xi \rightarrow \infty$; $\partial\psi/\partial\xi = E\sin\theta$. In the inflow region; $\omega = 0$ and $\phi = 0$. In the outflow region; $\partial\omega/\partial\xi = 0$ and $\partial\phi/\partial\xi = 0$;

(3) plane of symmetry, i.e. $\eta = 0$ and $\eta = 1$; $\psi = \omega = \partial\phi/\partial\eta = 0$; and

(4) on the fin surface; $\psi = 0$, $\omega = (1/E^2)(\partial^2\psi/\partial\eta^2)$, and $\phi_{ij} = 1.0$.

The system of elliptic PDEs given by equations (14)-(16) along with the corresponding boundary conditions was discretized using the finite difference method. The resulting system of algebraic equations was solved using the hybrid scheme (Patankar, 1980). Such a method proved to be numerically stable for convection-diffusion problems. The finite difference form of the equations was checked for consistency with the original PDEs (Patankar, 1980). The iterative solution procedure was carried out until the error in all solution variables (ψ,ω,ϕ) became less than a predefined error level ($\in$). Other predefined parameters needed for the solution method included the placement of the far-stream boundary condition (R_∞) and the number of grid points in both radial and tangential directions, N and M, respectively. Extensive testing was carried out in order to determine the effect of each of these parameters on the solution. This was done to ensure that the solution obtained was independent of and not tainted by the predefined value of each of these parameters. The testing included varying the value of $\in$ from 10^{-3} to 10^{-6}, R_∞ from 5 to 50, N from 100 to 200, and M from 100 to 140. The results reported herein are based on the following combination: $N = 189$, $M = 120$, $R_\infty = 25$, and $\in = 10^{-5}$.

In the previous work for uniformly spaced fins (Abu-Hijleh, 2003), the number of grid points was varied in the radial and tangential directions in order to ensure that all fins coincided with one of the grid's radial lines and that the fins end coincided with one of the grid's tangential lines (Figure 2). The need for the fins to coincide with the grid was also observed in this study but in a different fashion. In order to avoid any changes that might result from using different grids for different combinations of number fin(s) and fin height, a fixed grid size (189×120) was used for all combinations in this study. In this study the fin's tangential location was varied in 15° increments between 15 and 165°. Thus using $M = 120$ insured that the tangential grid resolution was suitable for all tangential fin locations. The hardest part was adjusting the radial grid resolution to ensure that the fin's end coincided with one of

the radial grid points. In this study the nominal fin height (H) used was: 0.25, 0.5, 1.0, 1.5, and 2.0. The combination of $N = 189$ and $R_\infty = 25$ resulted in a difference of less than 1 per cent between the actual fin height and the nominal fin height used in the current study. The actual height being that of the fin used in the calculation with its end coinciding with the closest radial grid point while using a fixed radial grid resolution ($N = 189$). The current gird resolution is finer than most grid resolutions used in published studies of natural (Saitho *et al.*, 1993), forced convection from a heated cylinder (Ahmad, 1996), and mixed convection at different angles of attack (Abu-Hijleh, 1999). The large number of grid points in the tangential direction ($M = 120$) was to ensure that there were sufficient grid points between the fins to properly resolve the flow between the fins, even when using 11 fins. In comparison, the use of 60 points in the tangential direction would have been sufficient to resolve the flow around a smooth cylinder (Abu-Hijleh, 1999). Figure 3 shows very good agreement between the profiles of the average Nusselt number calculated by the current code and several results reported in the literature (Ahmad, 1996; Abu-Hijleh, 1999; Incropera and DeWitt, 1996; Badr, 1980), for the case of a smooth cylinder, i.e. no fins.

Results

The effect of fins on the forced cross-flow heat transfer from a horizontal isothermal cylinder was studied for several combinations of number of fins ($F = 1, 2, 3, 5, 6, 11$), non-dimensional fin height ($H = 0.25, 0.5, 1.0, 1.5, 2.0$), and Reynolds number ($\mathrm{Re}_D = 5, 20, 70, 150$). The change in the average Nusselt number, for a given value of Reynolds number, due to the addition of F number of fin(s) ($\overline{\mathrm{NU}}_{D,F}$) was normalized by the Nusselt number of a smooth cylinder, no fins, at the same Reynolds number ($\overline{\mathrm{NU}}_D$). This was done in order to focus on the relative effect of adding the fins ($\overline{\mathrm{NU}}_{D,F}$).

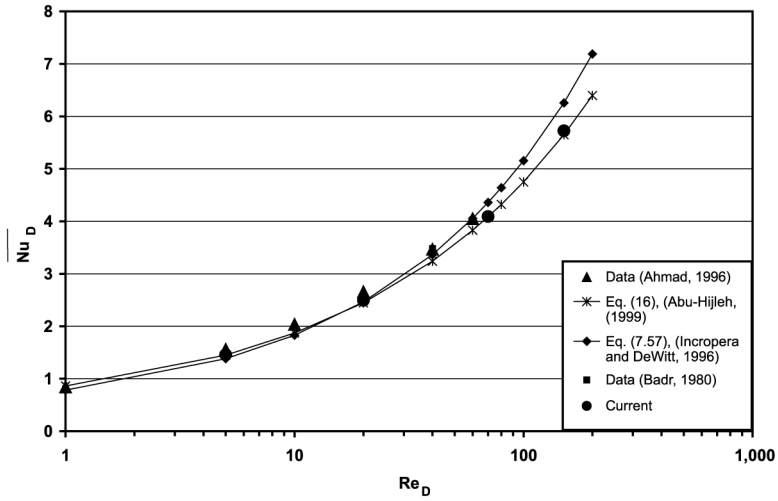

Figure 3.
Comparison of the local Nusselt number for the case of a smooth cylinder. The equations' numbers are from their respective references

The presence of the fins has an effect on both the aerodynamic as well as the thermal characteristics of the flow. The fins tend to obstruct the airflow near the cylinder surface, thus reducing the heat transfer from the cylinder's surface to the surrounding fluid. On the other hand, the fins increase the heat transfer area resulting in an increase in the heat transfer from the cylinder to the surrounding fluid. The net result of these two opposing effects depends on the combination of number of fins, fin height, and Reynolds number. Detailed results and discussion of these changes for the case of uniformly spaced fins can be found in a previous work by the author Abu-Hijleh (2003). For completeness and as a reference, some of the uniformly spaced cases were repeated in this study. Figure 4 shows the changes in the $\overline{\mathrm{NU}}_{D,F}$ as a function of the number of uniformly spaced fins of different heights for the Reynolds number values covered in this work. The results of the uniformly spaced fins were used to establish the maximum increase in Nusselt number that can be achieved by using uniformly spaced fins. These values served as the reference for the assessment of the effectiveness of fin placement optimization. Figure 4 already shows that there is an optimal number of fins beyond which the Nusselt number will not increase or even decrease. The use of short fins, $H \leq 0.5$, tended to result in a lower Nusselt number than for the case without any fins, especially at low Reynolds numbers. The short fins significantly disrupted the airflow around the cylinder and created a buffer between the free stream and the cylinder surface (Figure 5). This resulted in a significant drop in heat transfer from the cylinder surface. The extra heat transfer area due to the addition of short fins, and resulting additional heat transfer to the surrounding fluid was small and did not compensate for the reduction of heat transfer from the cylinder surface. One result from this figure that will be used in the optimization part is the value of the maximum normalized Nusselt number that can be achieved using uniformly spaced fins and the number of those fins. For cases where the use of any number of fins resulted in a reduction in the Nusselt number, the Nusselt number value that will be used will be that of the smooth cylinder, i.e. $F = 0$. For example, at $\mathrm{Re}_D = 70$ and $H = 0.25$, the maximum value of normalized Nusselt number will be 1.0 achieved at $F = 0$. The use of this value will become clearer in the next paragraph.

The first part of the optimization process was to see the changes in the Nusselt number as a function of the tangential location of a single fin. Figure 6 shows the change in $\overline{\mathrm{NU}}_{D,F}$ as a function of the tangential location of a single fin of different heights at different Reynolds numbers. The tangential location was changed from 15 to 165 in 15° increments. Note that the direction of the x-axis has been reversed in order to match the schematic shown in Figure 1. A small insert showing the cylinder and direction of the incoming flow is also shown in this figure. The same format applies for subsequent figures as noted in their respective captions. The $\overline{\mathrm{NU}}_{D,F}$ value shown at 180° is the maximum value obtained using uniformly spaced fins, based on the results shown in Figure 4, with the corresponding number of fins used shown next to those points. Two conclusions can be drawn form this figure. First, a properly placed single fin can result in a $\overline{\mathrm{NU}}_{D,F}$ value higher than that obtained from using the optimal number of uniformly spaced fins. This was the case for all combinations of $\mathrm{Re}_D \geq 70$ and $H \geq 0.5$. This is the first indication that optimization of the tangential placement of the fin(s) is important. Figure 6 also gives an idea as to the locations where the fin placement is most effective, even in cases where the single fin did not

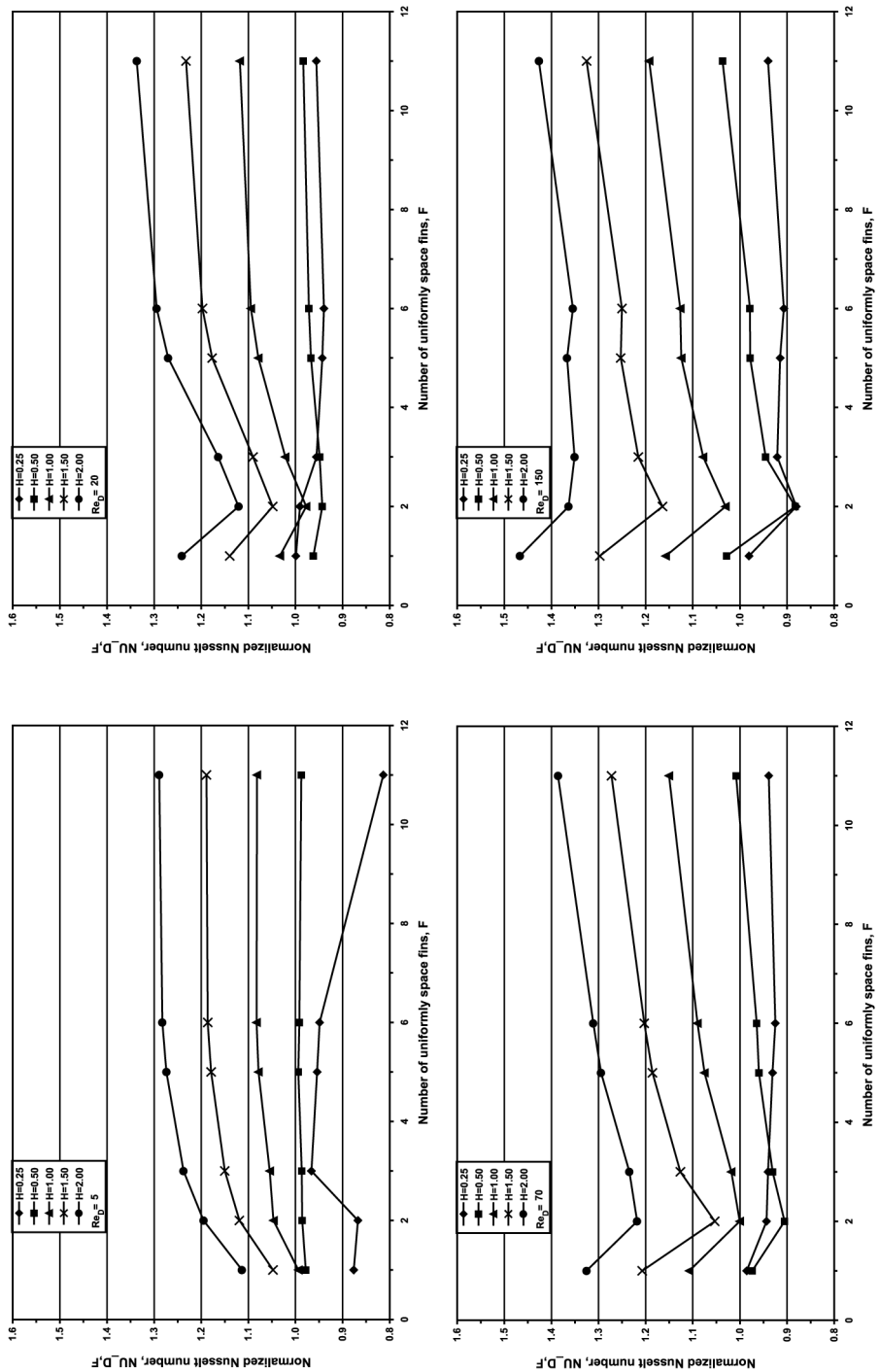

Figure 4.
Normalized average Nusselt number as a function of the number of uniformly spaced fins at different combinations of fin height and Re_D

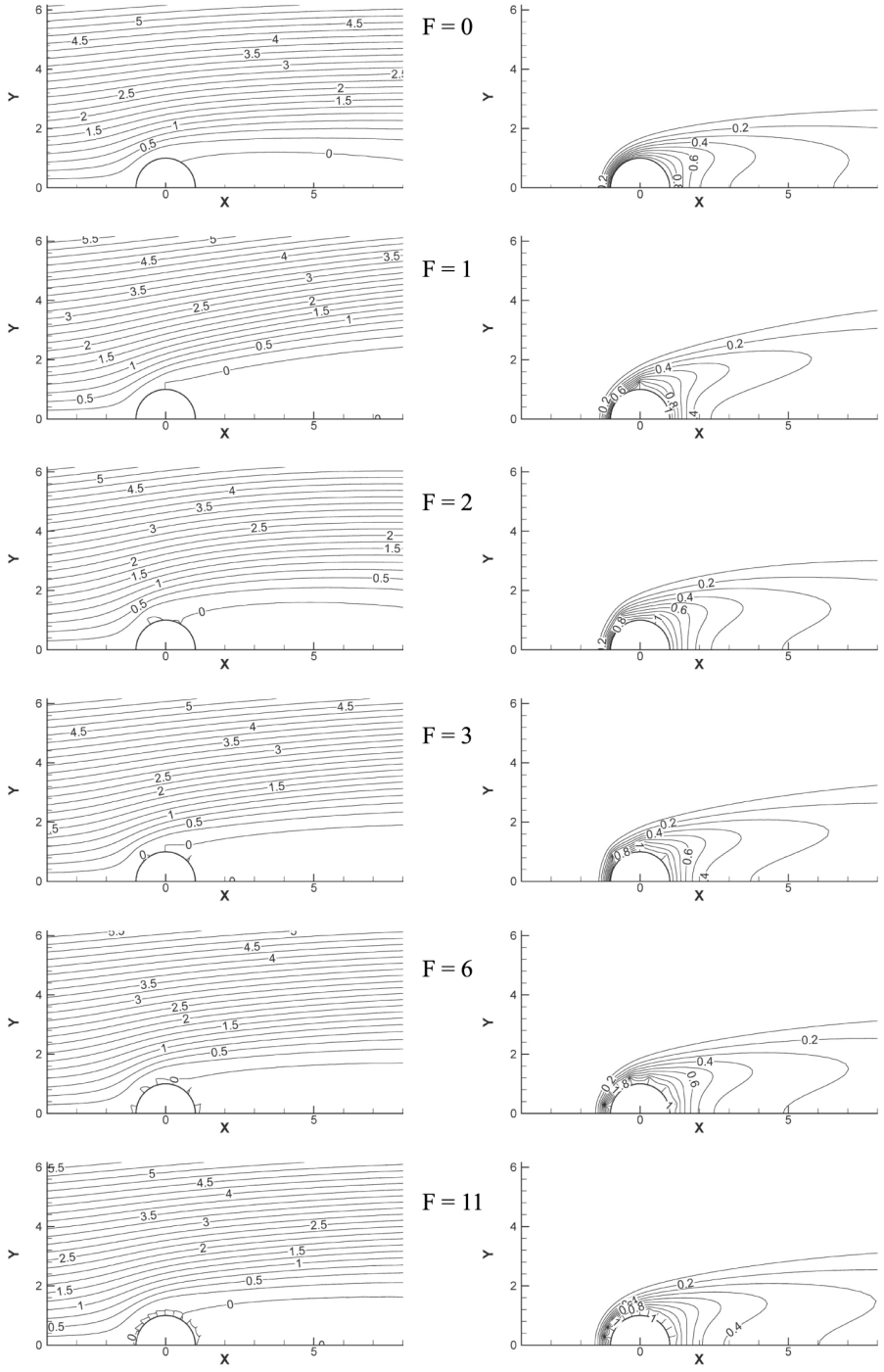

Figure 5.
Streamlines (left) and isothermal (right) counters at different values of uniformly spaced fins, for the case of Re_D=70 and $H = 0.25$

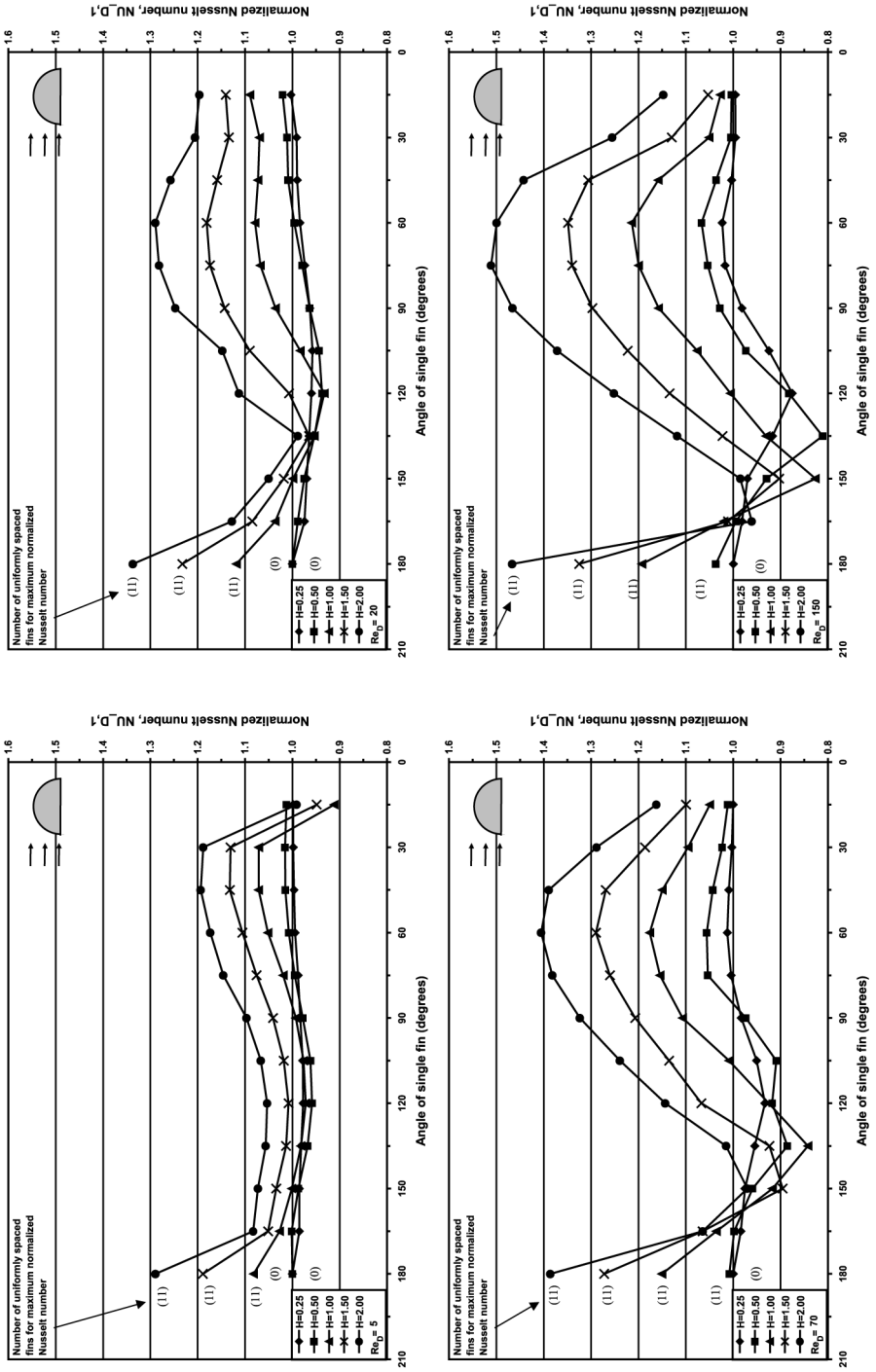

Figure 6.
Change of the normalized average Nusselt number as a function of the tangential location using a single fin. Direction of *x*-axis reversed to comply with direction shown in Figure 1

result a $\overline{NU_{D,F}}$ higher than that obtained using the optimal number of uniformly spaced fins. The values of these "best" single fin tangential locations are listed in Table I for all Reynolds number and fin height combinations. The best location for a single fin seems to be at or around the point of flow separation for the case of a smooth cylinder. Figure 7 shows the tangential distribution of the local vorticity and Nusselt number along the surface of a smooth cylinder. Since the cylinder wall is assumed to be impermeable, there is no radial velocity at the cylinder surface ($U = \partial\psi/\partial\theta = 0$). Since this condition applies along the entire surface of the cylinder, then the tangential gradient of the radial velocity at the cylinder surface will also be zero ($\partial U/\partial\theta = \partial^2\psi/\partial\theta^2 = 0$). Given this condition, and from the vorticity definition in equation (14), the vorticity at the cylinder wall is equivalent to the radial gradient of the tangential velocity component along the cylinder surface ($\omega_0 = \partial V/\partial\xi = \partial^2\psi/\partial\xi^2$). Thus a wall vorticity value of zero is equivalent to flow separation at the cylinder surface. The distribution of the wall vorticity in Figure 7 shows the tangential locations of the flow separation for the case of a smooth cylinder at different values of Reynolds number. Note that there is no separation for the case of $Re_D = 5$. This correlation between the separation point and the best location of a single fin can be explained by the fact that most of the heat transfer from the surface of a smooth cylinder occurs at the "front" of the cylinder, i.e. the region before separation (Figure 7). Thus adding a fin around that location would result in minimal reduction in the heat transfer from the front of the cylinder while providing additional heat transfer area. Having the fin located near the point of separation and not further toward the back of the cylinder means that the fin will also extend further into the cold incoming airflow, which increases the temperature differential and resulting heat transfer. If the fin is placed further toward the back of the cylinder it will be in the relatively hot and low velocity recirculation region which would make the fin less "productive" due to the smaller temperature differential between the fin and the surrounding fluid. This can been seen from the local Nusselt distribution as well as the streamline and isothermal contours in Figure 8 for the cases of $Re_D = 70$, $H = 2.0$, $F = 1$, and $\theta = -, 15, 60, 150$.

Figure 9 shows the change in $\overline{NU_{D,F}}$ for the case of two non-uniformly spaced fins, of equal height, at different values of Reynolds number. In this figure, one fin was fixed at best tangential location of a single fin, as per Table I, while the tangential location of the second fin was varied from 15 to 165°, bypassing of course the location of the fixed fin. For the most part, using two fins resulted in a normalized Nusselt number similar to that of the maximum obtained using a single fin. The values of these "best" second fins tangential locations are listed in Table II for all Reynolds number and fin height combinations. At high values of Reynolds number and long fins, $Re_D \geq 70$ and

Table I.
Best tangential location for maximum $\overline{NU_{D,1}}$ when using a single fin

Reynolds number (Re_D)	Non-dimensional fin height (H)				
	0.25	0.5	1.0	1.5	2.0
5	15	30	45	45	45
20	15	15	15	60	60
70	60	60	60	60	60
150	60	60	60	60	75

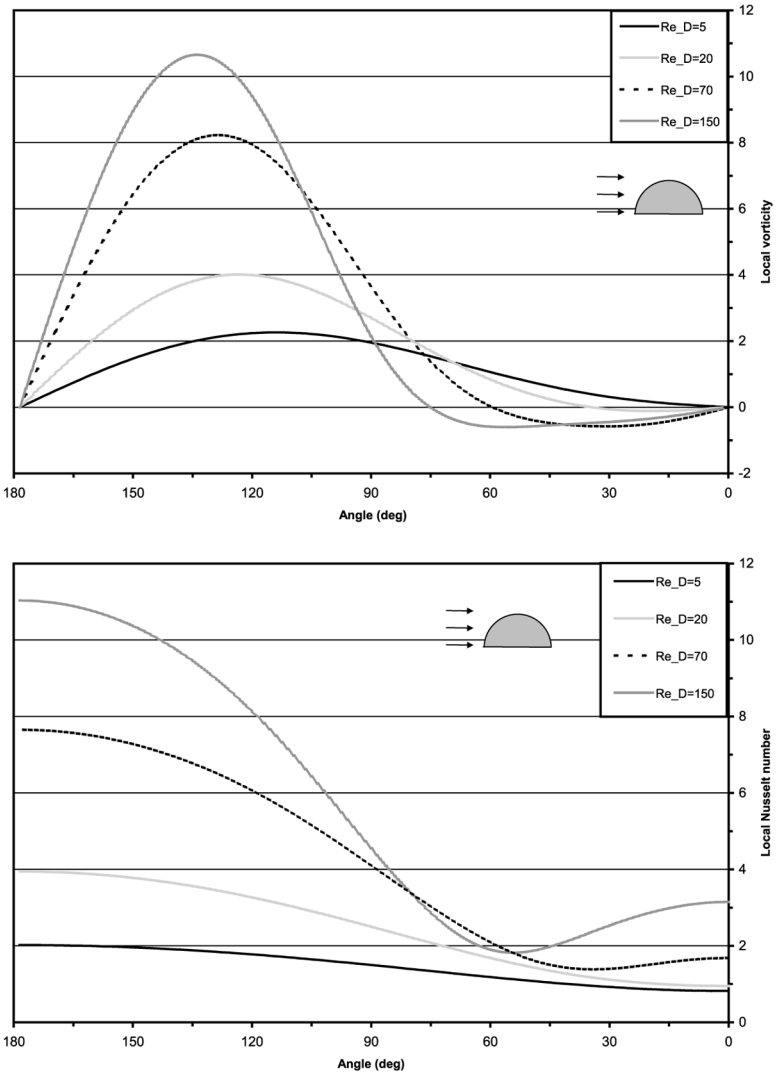

Figure 7.
Variation of the local vorticity (top) and Nusselt number (bottom) along the cylinder's wall for the case of smooth cylinder. Direction of x-axis reversed to comply with direction shown in Figure 1

$H \geq 1.0$, the $\overline{\mathrm{NU}_{D,F}}$ values from a single fin were equal to or better than all combinations of two non-uniformly spaced fins as well as the highest value obtained using uniformly spaced fins. The addition of the second fin increased the heat transfer area but further disrupted the flow around the cylinder surface. The best location for the second fin tended to be at either the very front or back of the cylinder where it resulted in the least disruption to the flow around the cylinder. Other location of the second fin resulted in significant flow disruptions that outweighed the additional heat transfer area. Also placing the second fin ahead of the first fixed fin resulted in a significant reduction in the contribution of the fixed fin as it fell in the immediate wake

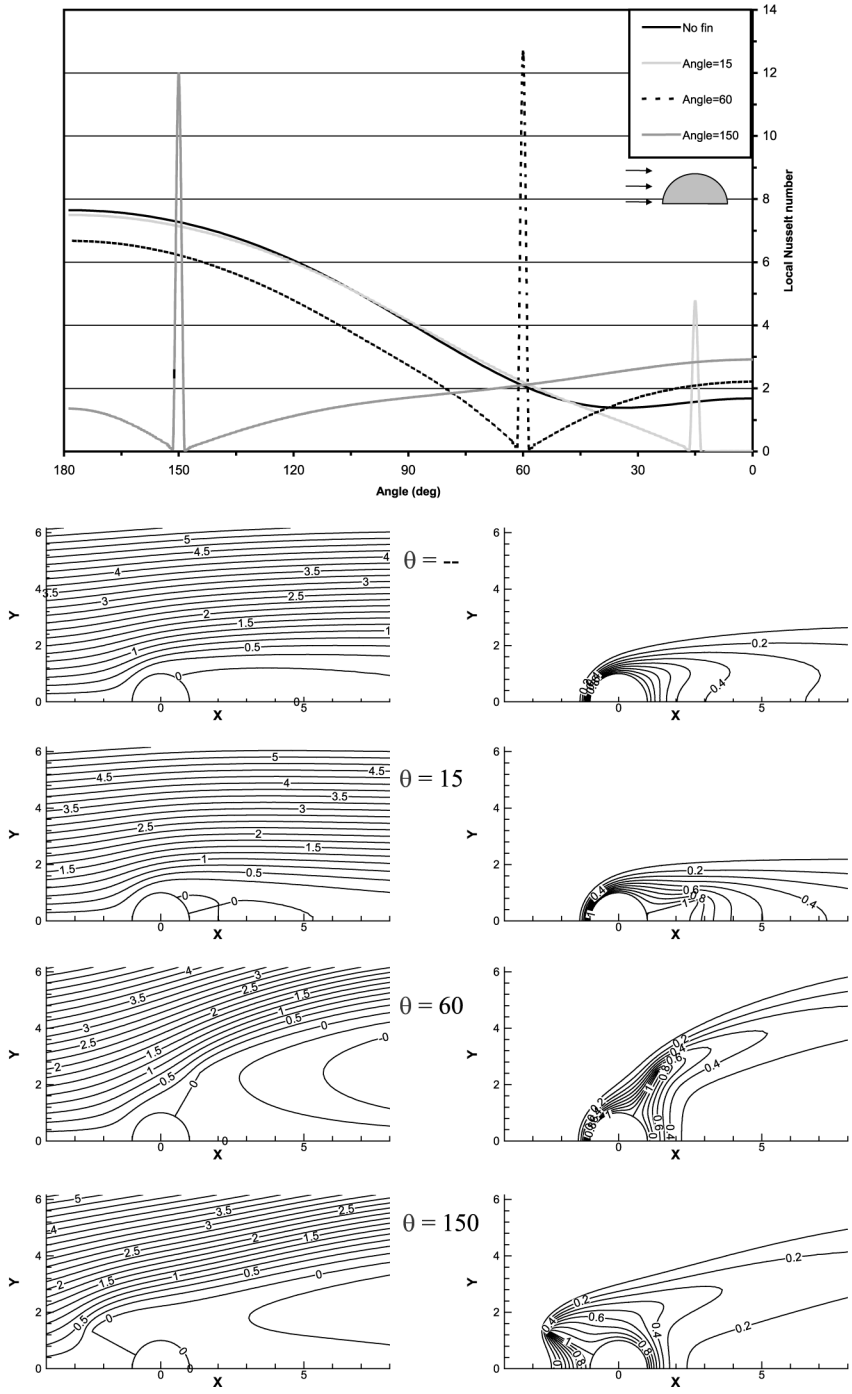

Figure 8.
Local Nusselt number distribution along the cylinder surface (top) and the streamline (bottom left) and isothermal (bottom right) contours for the case of $Re_D = 70$, $H = 2.0$, $F = 1$, and $\theta = -$, 15, 60, and 150

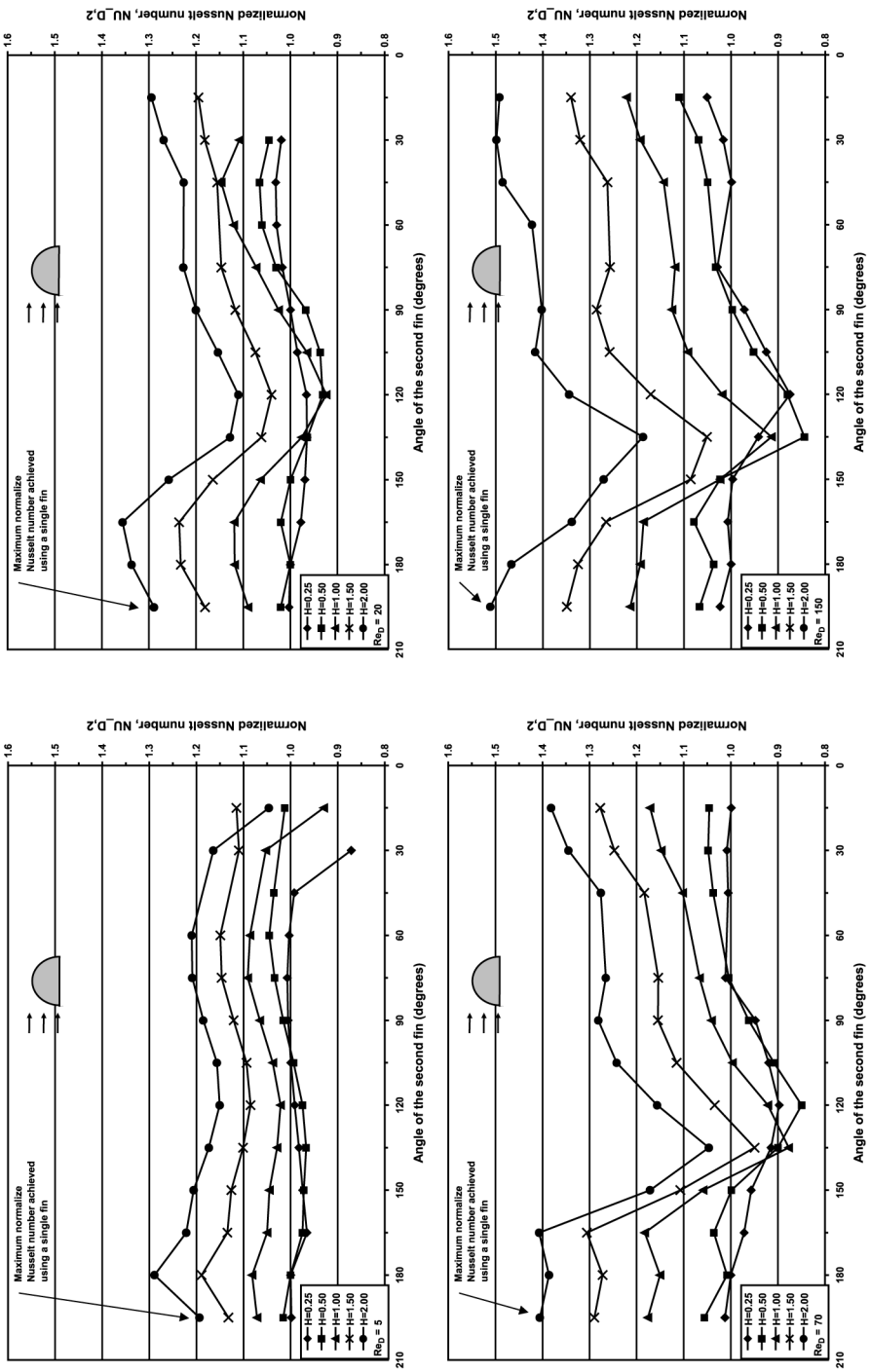

Figure 9.
Change of the normalized average Nusselt number as a function of the tangential location using two fins. Direction of *x*-axis reversed to comply with direction shown in Figure 1

of the second upstream fin, e.g. when the second fin was located at $\theta_2 = 135°$. This was not the case when the second fin as located behind the fixed fin or at the very front of the cylinder, $\theta_2 = 15$ and 165, respectively. Figure 10 shows the local Nusselt distribution as well as the streamline and isothermal contours for the case of $\mathrm{Re}_D = 70$, $H = 2.0$, $F = 2$, and angle of the second fin $(\theta_2) = -, 15, 135, 165$. In this figure, the first fin is fixed at the best tangential location of a single fin as given in Table I, i.e. $\theta_1 = 60$.

Figure 11 shows the two fins "cost-efficiency" (η_{fc}) as a function of the tangential location of the second fin. Also included in the figure are the η_{fc} for the combinations of uniformly spaced fins and a single fin that resulted in the maximum normalized Nusselt number for each arrangement, from Figures 4 and 6. The general trend is that when using long fins, $H \geq 1.0$, a properly positioned fin tends provides the best return in terms of enhanced heat transfer per fin cost. For shorter fins, $H \leq 0.5$, the use of two properly positioned fins tends provides the best return in terms of enhanced heat transfer per fin cost. Comparing Figures 6, 9, and 11 shows that the fin(s) combination that results in the highest normalised Nusselt number is not always the same combination that results in the highest fin "cost-efficiency". Thus it is important to establish the relative priority of enhanced heat transfer requirements versus the economic return of using fins before making a decision as to the number of fins to be fitted to a cylinder.

Conclusions

The problem of cross-flow forced convection heat transfer from an isothermal horizontal cylinder with high conductivity fins was studied numerically. Changes in the normalized average Nusselt number at different combinations of number of fins, fin height, fin(s) tangential location, and Reynolds number were reported. The results indicated that the optimal configuration consists of using one or two fins, depending on the fin height and Reynolds number. The best position of the first fin is around the point of separation for the case of a smooth cylinder. The best position of the second fin, for the two-fin configurations, is either toward the very front or back of the cylinder. The fin cost-efficiency was also studied and showed that the configuration with the highest fin cost-efficiency did not always coincide with that resulting in the maximum Nusselt number. The results can be used to design highly efficient cross-flow forced convection heat transfer configurations from a horizontal cylinder with minimum cost.

Table II.
Best tangential location of the second fin for maximum $\overline{\mathrm{NU}_{D,2}}$ when using two fins. Angle of first fin fixed at value shown in Table I

	Non-dimensional fin height (H)				
Reynolds number (Re_D)	0.25	0.5	1.0	1.5	2.0
5	75	60	75	60	165
20	45	45	45	15	165
70	75	30	165	165	165
150	15	15	15	15	30

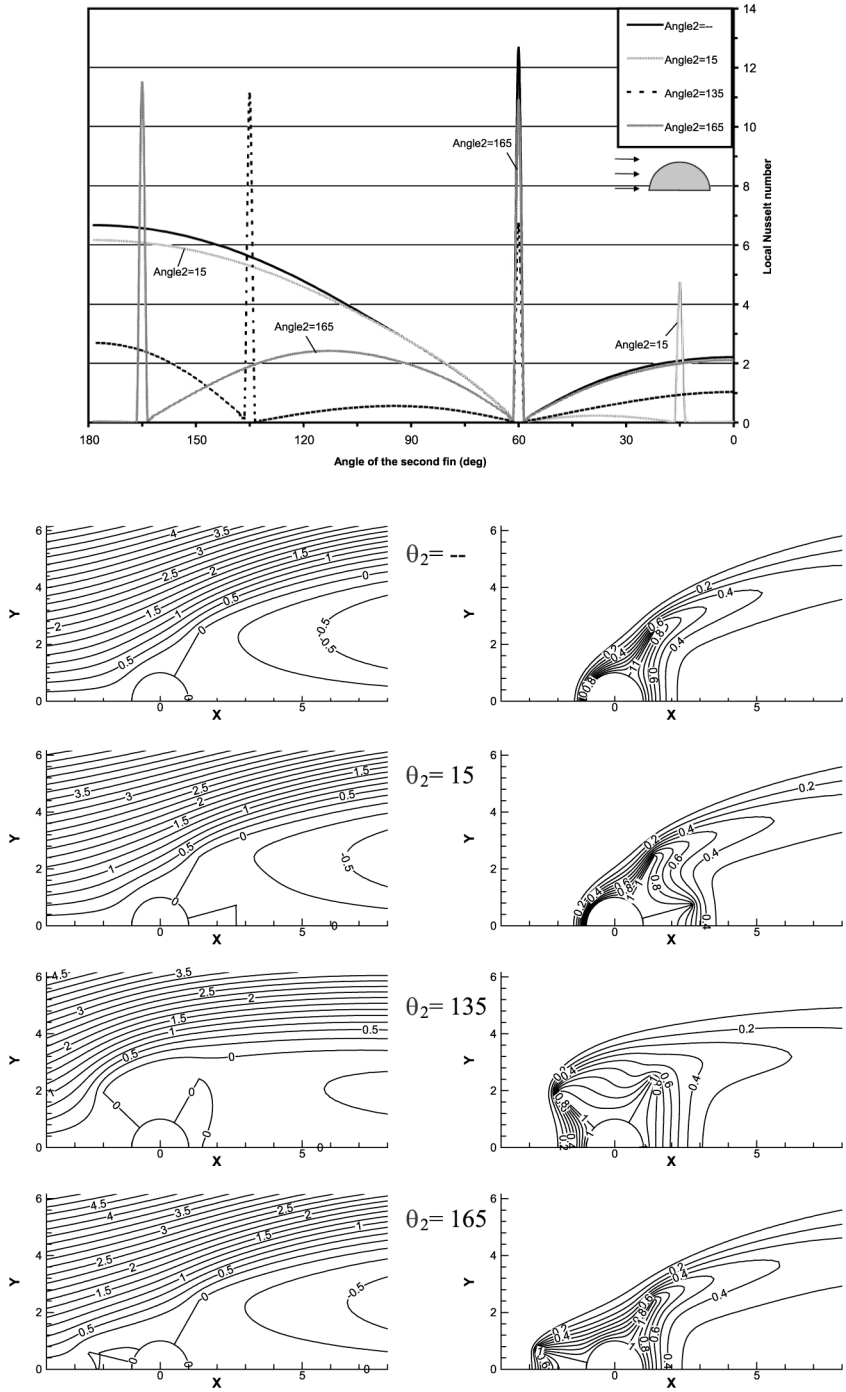

Figure 10.
Local Nusselt number distribution along the cylinder surface (top) and the streamline (bottom left) and isothermal (bottom right) contours for the case of $Re_D = 70$, $H = 2.0$, $F = 2$, and $\theta_2 = -$, 15, 135, and 165

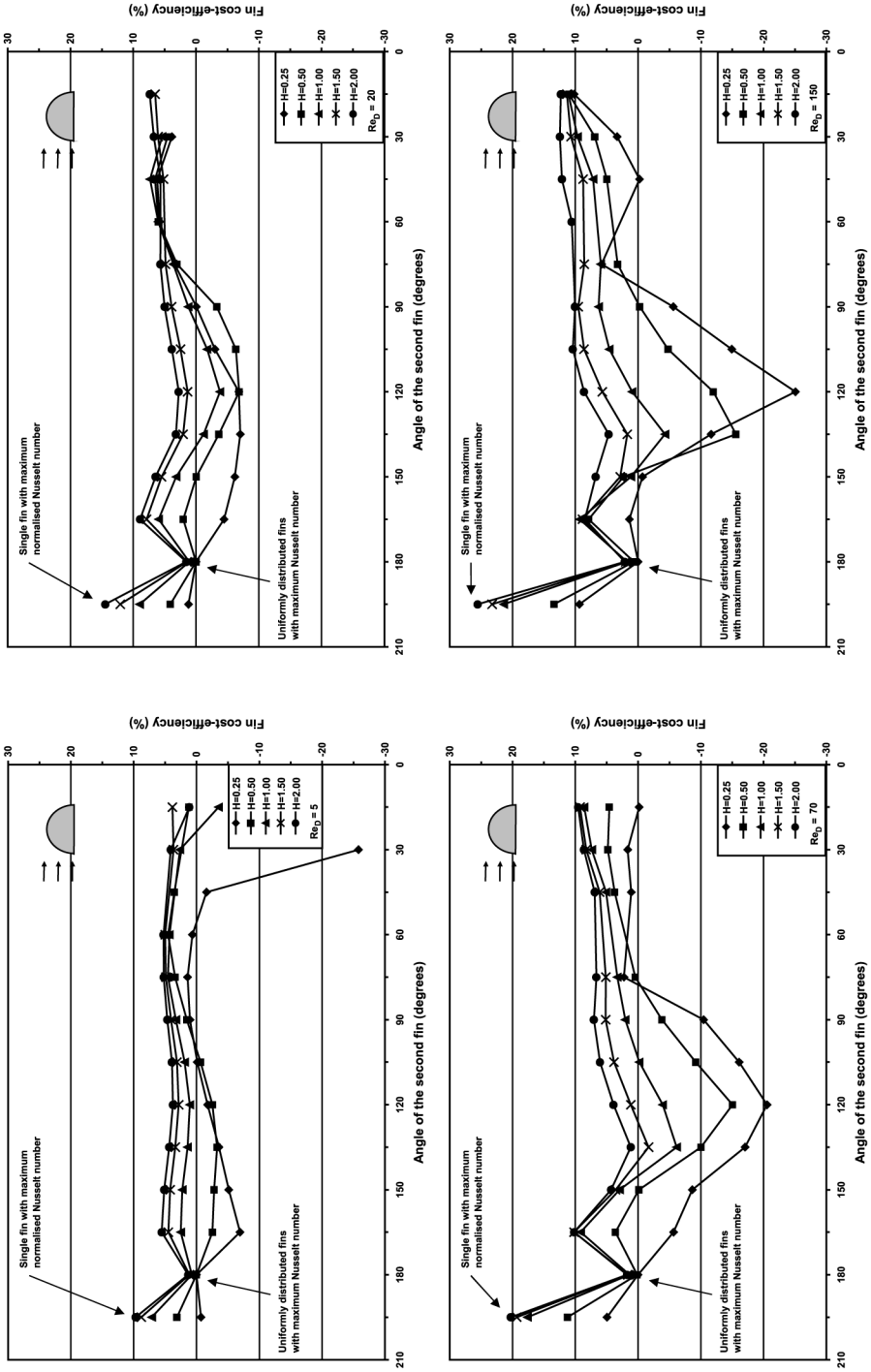

Figure 11.
Change of fin cost-efficiency as a function of the tangential location of the second fin. Direction of x-axis reversed to comply with direction shown in Figure 1

References

Abu-Hijleh, B.A/K. (1999), "Laminar mixed convection correlations for an isothermal cylinder in cross flow at different angles of attack", *Int. J. Heat Mass Transfer*, Vol. 42, pp. 1383-8.

Abu-Hijleh, B.A/K. (2001), "Natural convection heat transfer from a cylinder covered with an orthotropic porous layer", *Numerical Heat Transfer*, Vol. 40, pp. 405-32.

Abu-Hijleh, B.A/K. (2003), "Numerical simulation of forced convection heat transfer from a cylinder with high conductivity radial fins in cross-flow", *Int. J. Thermal Sciences*, Vol. 42 No. 8, pp. 749-57.

Ahmad, R.A. (1996), "Steady-state numerical solution of the Navier-Stokes and energy equations around a horizontal cylinder at moderate Reynolds numbers from 100 to 500", *Heat Transfer Engineering*, Vol. 17, pp. 31-81.

Al-Nimr, M.A. and Alkam, M.K. (1998), "A modified tubeless solar collector partially filled with porous substrate", *Renewable Energy*, Vol. 13, pp. 165-73.

Anderson, J.D. (1994), *Computational Fluid Dynamics: The Basics with Applications*, McGraw-Hill, New York, NY.

Badr, H.M. (1980), "A theoretical study of laminar mixed convection from a horizontal cylinder in a cross stream", *Int. J. Heat Mass Transfer*, Vol. 26, pp. 639-53.

Incropera, F.P. and DeWitt, D.P. (1996), *Fundamentals of Heat and Mass Transfer*, Wiley, New York, NY.

Patankar, S.V. (1980), *Numerical Heat Transfer and Fluid Flow*, McGraw-Hill, New York, NY.

Saitoh, T., Sajik, T. and Maruhara, K. (1993), "Benchmark solutions to natural convection heat transfer problem around a horizontal circular cylinder", *Int. J. Heat Mass Transfer*, Vol. 36, pp. 1251-9.

Vafai, K. and Huang, P.C. (1994), "Analysis of heat transfer regulation and modification employing intermittently emplaced porous cavities", *J. Heat Transfer*, Vol. 116, pp. 604-13.